ACS Catalysis

Research Article

pubs.acs.org/acscatalysis

Factors Impacting the Mechanism of the Mono-N-Protected Amino Acid Ligand-Assisted and Directing-Group-Mediated C−H Activation Catalyzed by Pd(II) Complex

Brandon E. Haines and Djamaladdin G. Musaev*

Cherry L. Emerson Center for Scientific Computation, Emory University, 1515 Dickey Drive, Atlanta, Georgia 30322, United States

Supporting Information

ABSTRACT: We computationally studied the roles of the (a) protecting group (PG), (b) side chain (R), and (c) length of amino acid backbone of the mono-N-protected amino acid (MPAA) ligand as well as (d) the nature of the substrate (DG-SUB) and directing group (DG) on the following elementary steps of the "N−H bond cleavage and subsequent C−H bond activation" mechanism for [MPAA]−Pd(II)-catalyzed C−H activation: (i) formation of the prereaction complex, [MPAA]−Pd(II)−[DG-SUB], with a weakly coordinated monoanionic amino acid ligand; (ii) N−H bond cleavage and formation of the catalytically active intermediate, [MPAA′]−Pd(II)−[DG-SUB], with a bidentately coordinated dianionic amino acid ligand, and (iii) C−H bond activation in [MPAA′]−Pd(II)−[DG-SUB] occurring via the concerted metalation/deprotonation pathways A (outer-sphere) and B (inner-sphere). For the prereaction complex, we find that weak coordination of the MPAA ligand to Pd(II) is affected by (a) the strong electron-withdrawing ability of the PG, (b) longer amino acid backbone, and (c) a strong Pd-DG interaction. For the N−H bond-cleavage step, we find that facile N−H cleavage is affected by (a) the strong electron-withdrawing ability of the PG, (b) the existence of stabilizing noncovalent interactions, and (c) a weak Pd−DG interaction. For the C−H activation step, we report that (a) the increase in the electron-withdrawing ability of the PG stabilizes both pathways A and B, whereas proton affinity of the PG impacts only pathway B; (b) the geometrical features of the substrate−ligand motif in [MPAA′]−Pd(II)−[DG-SUB] and the existence of stabilizing noncovalent interactions can alter the reaction mechanism; and (c) the enantioselectivity of the reaction is reported to be controlled by either steric congestion around the substrate (in pathway A) or cooperative ligand-substrate geometrical constraints (in pathway B).

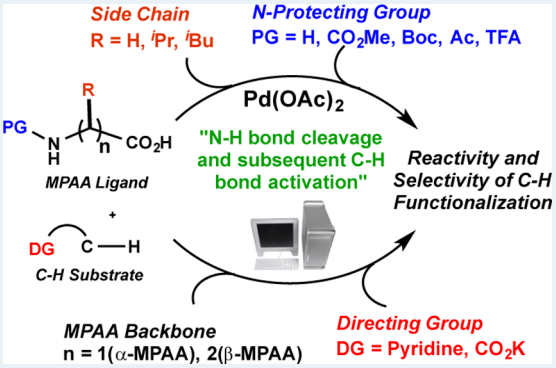

KEYWORDS: *C−H functionalization, protecting group, directing group, Pd catalyst, mono-N-protected amino acid ligand, weak interactions, computational study*

1. INTRODUCTION

An emerging appreciation for the synthetic utility of C−H bonds as functional groups and their ubiquitous nature have led to the development of transition-metal-catalyzed C−H functionalization as a powerful strategy to expand access to important pharmaceutical compounds and novel materials.[1] However, it remains a challenge to develop highly efficient catalysts with excellent stereo-, regio-, and chemoselectivity. One of the incipient approaches to meet these challenges is the use of a directing group (DG) strategy that brings the targeted C−H bond in greater proximity to the transition metal center so that it can activate the C−H bond and form the reactive metal−alkyl/aryl intermediate.[2] However, suitable ligand scaffolds are required to stabilize the resulting metal−alkyl/aryl intermediates and make them synthetically useful. Recently, Yu and co-workers made the seminal discovery that the addition of mono-N-protected amino acid ligands (MPAA) to $Pd(OAc)_2$ effectively stabilizes the reactive [Pd(II)-R] intermediate (formed after the directing-group-mediated C−H bond activation) and promotes $Pd(OAc)_2$-catalyzed C−H functionalization of 2-benzhydrylpyridine (referred to as PYR), 2-(2-(trifluoromethyl)phenyl)acetic acid (referred to as PAA) and *N*,*N*-bis(2-cyanophenyl)-3-phenylpropanamide (referred to as MCN) (see Scheme 1).[3]

Currently, MPAAs represent an important class of ligand scaffold that stabilize the [MPAA]−Pd(II)−[DG-SUB] structural motif and facilitate selective functionalization of the $C(sp^2)$−H and $C(sp^3)$−H bonds of numerous substrates (DG-SUB).[4] Extensive studies on the role of the MPAA ligand in these systems have allowed for the expansion of the scope of DGs (and consequently, the scope of the substrates, SUB) to carbonyls, ethers, nitriles, and other synthetically useful groups.[3b,5] Furthermore, these studies have demonstrated that the nature of the side chain (R), length of amino acid backbone,

Received: September 26, 2014
Revised: December 15, 2014
Published: December 17, 2014

DOI: 10.1021/cs5014706
ACS Catal. 2015, 5, 830−840

Scheme 1. Relevant Examples of the MPAA-Assisted and DG-Mediated C−H Bond Functionalization Catalyzed by $Pd(OAc)_2$ That Illustrate the Effect of the N-Protecting Group on the Reaction

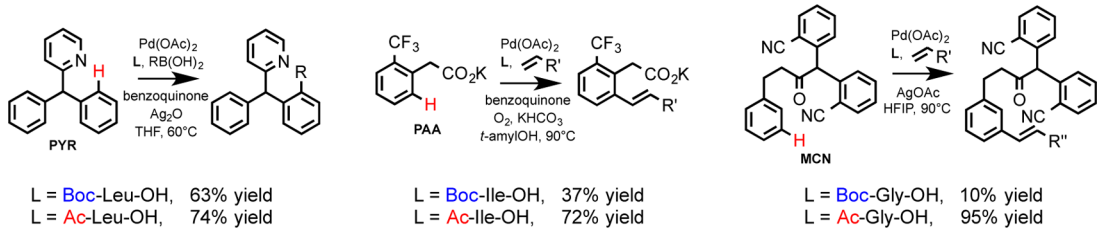

L = Boc-Leu-OH, 63% yield
L = Ac-Leu-OH, 74% yield

L = Boc-Ile-OH, 37% yield
L = Ac-Ile-OH, 72% yield

L = Boc-Gly-OH, 10% yield
L = Ac-Gly-OH, 95% yield

and N-protecting group (PG) (see Scheme 1) of the MPAA ligand play a crucial role in determining the reactivity and selectivity of the [MPAA]−Pd(II)-catalyzed C−H bond functionalization and subsequent C−C and C-heteroatom formation. Gratifyingly, these parameters of the inexpensive MPAA ligand scaffold are extensively modifiable. For example, Yu and co-workers have shown that substitution of a -Boc protecting group with -Ac enhances C−H bond functionalization in PYR, PAA, and MCN substrates (for example, see Scheme 1). Other reported alterations to the MPAA ligand scaffold include cyclopropane derivatives and replacing the carboxy terminus with an *O*-methyl hydroxamic acid (MPAHA).[6] The available experiments also show that the nature of the activated C−H bond (sp^2 vs sp^3) and Pd−DG interaction are other vital factors impacting the reactivity and selectivity of C−H bond in the [MPAA]−Pd(II)−[DG-SUB] complex.

Recently, Musaev, Yu, and co-workers have studied the mechanism of the enantioselective C−H bond activation in [Boc-Val-O]−Pd(II)−[PYR] using both computational and experimental approaches and have predicted the "N−H bond cleavage and subsequent C−H bond activation" mechanism for this reaction (see Scheme 2).[7] These studies have demonstrated that the MPAA ligand, that is, Boc-Val-O−, plays multiple roles during the reaction. It acts as (i) a weakly coordinated monoanionic ligand that stabilizes the [MPAA]−Pd(II)−[PYR] precatalyst, **I1**; and (ii) a soft electron donor (from the N-terminus) and bidentately coordinated dianionic ligand that forms the catalytically active [MPAA′]−Pd(II)−[DG-SUB] intermediate, **I2** (or **I3**), where MPAA′ stands for the deprotonated MPAA ligand. The resulting intermediate can then undergo arene C−H bond activation via the outer-sphere (or external-acetate-assisted) concerted metalation−deprotonation (CMD) mechanism to form a new Pd-aryl bond in the product palladacycle, **P** (see Scheme 2, pathway A).[5i,k,8] Ensuing studies by Wu, Houk, Yu and co-workers[9] as well as Musaev and co-workers[7a] showed that the bidentately coordinated dianionic ligand (MPAA′) can also act as the proton acceptor for arene C−H bond activation via the inner-sphere (or internal-acetate-assisted) CMD mechanism (see Scheme 2, pathway B). For PYR, the formation of the experimentally observed *R* product is reported to be kinetically favored by 1.8 and 6.3 kcal/mol for the outer-sphere (A) and inner-sphere (B) pathways, respectively.[7] Interestingly, during the C−H activation, the Pd-center acts as a coordinatively flexible metal center that holds the substrate and amino acid ligand in close vicinity to promote the chemical transformation.

These computational findings are consistent with the competition experiments by Yu and co-workers suggesting that the amino acid ligands are not merely enhancing the TON (turnover number) but also are generating a more reactive

Scheme 2. Schematic Presentation of the "N−H Bond Cleavage and Subsequent C−H Bond Activation" Mechanism of the MPAA-Assisted and Directing-Group-Mediated C−H Activation Catalyzed by $Pd(OAc)_2$ Complex

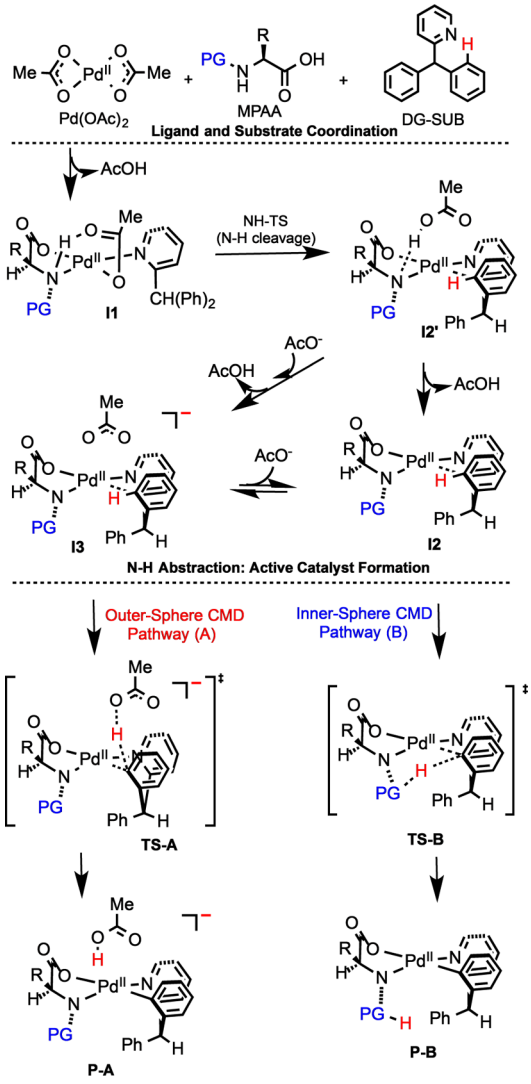

catalyst.[3c] Furthermore, these findings were supported by (1) the detailed kinetic analysis of the $Pd(OAc)_2$-catalyzed C−H bond olefination in the presence of MPAA ligands (such as Ac-Ile-O−, Ac-Val-O−, Boc-Val-O−, and Boc-Ile-O−) showing that the determined overall kinetic rate law holds if the formation of two kinetically indistinguishable species, **I1** and **I2**, is assumed;[10] (2) mass-spectrometry and isotope pattern and fragmentation analysis via collision-induced dissociation detecting the bidentate [MPAA′]−Pd(II) complex in a mixture of

DOI: 10.1021/cs5014706
ACS Catal. 2015, 5, 830−840

$Pd(OAc)_2$ and *N*-acetyl-glycine (or *N*-Boc-glycine);[9] (3) DFT studies by Wu, Houk, Yu, and co-workers utilizing $Pd(OAc)_2$ and *N*-acetyl-glycine (i.e., MPAA) that show that deprotonation of the N−H bond of the MPAA ligand (i.e., MPAA → MPAA′ transformation) is highly favored and leads to the formation of a stable [MPAA′]−Pd(II)−[DG-SUB] complex;[9] and (4) other experimental and computational studies that find that N−H activation likely occurs prior to C−H activation, notably C−H functionalization utilizing an acidic amide DG.[11]

Comparison of the computational findings of Wu, Houk, Yu, and co-workers[9] with that of Musaev and co-workers[7] demonstrates, once again, the importance of the nature of the MPAA ligand and substrate on the mechanism of C−H activation in the [MPAA′]−Pd(II)−[DG-SUB] complex. Indeed, by utilizing $Pd(OAc)_2$ (as the catalyst), *N*-acetyl-glycine (as the MPAA ligand) and MCN (as the substrate) Houk and co-workers have found the inner-sphere C−H activation pathway (pathway B in Scheme 2) to be kinetically more favored than the outer-sphere C−H activation pathway (pathway A in Scheme 2) by 12.3 kcal/mol.[9] On the other hand, studies by Musaev and co-workers of the $Pd(OAc)_2$ (as a catalyst), *N*-Boc-valine (as a MPAA ligand) and PYR (as a substrate) have shown that the formation of the experimentally reported *R* product via the inner-sphere C−H activation pathway requires only 4.8 kcal/mol less energy barrier than the outer-sphere C−H activation pathway.[7a] One should mention that operation of the outer-sphere pathway A is expected to heavily rely on the reaction conditions such as base concentration, solvent, counterion, etc., whereas the inner-sphere pathway B depends more on the electronic and steric properties of the MPAA ligand (i.e., protecting group) and substrate (including Pd-DG interaction).

Thus, the existing studies point to the vast potential for the development of more efficient C−H functionalization reactions through more extensive alterations of both the MPAA scaffold and scope of DG-SUB. As such, a better understanding of the roles of each of the aforementioned factors will be crucial for the optimization of the reactivity and selectivity of DG-mediated [MPAA]−Pd(II)-catalyzed C−H bond functionalization. Because only limited mechanistic information can be obtained from experiments, it is imperative to utilize a complementary computational approach to gain more detailed insights into the aforementioned issues. In this paper, we elucidate the impact of the protecting group (PG = −H, $-CO_2Me$, −Boc, −Ac, and −TFA), side chain [R = H (i.e., Gly), ^{i}Pr (i.e., Val), and ^{i}Bu (i.e., Leu)], and length of amino acid backbone [*n* = 1 (*α*-amino acid) and 2 (*β*-amino acid)] of the MPAA ligand, as well as the nature of substrate (SUB = PYR and PAA) and the strength of the Pd−DG interaction (DG = pyridine and CO_2K), as summarized in Scheme 3, on the mechanisms of the following important elementary steps of the overall C−H activation reaction: (1) coordination of the MPAA ligand to Pd(II), leading to formation of prereaction complex **I1**; (2) N−H bond cleavage, leading to the formation of catalytically active intermediate **I2** (or **I3**); and (3) C−H bond activation via the pathways A (outer-sphere or external-acetate-assisted CMD) and B (inner-sphere or internal-acetate-assisted CMD), as shown in Scheme 2.[12] The obtained fundamental knowledge is expected to aid the development of novel MPAA−substrate combinations and strategies for the selective functionalization of C−H bonds of DG-SUB by utilizing $Pd(OAc)_2$ as a catalyst. It is important to note that the full catalytic C−H functionalization reactions also include several other elementary steps (for example, C−C and C−heteroatom bond coupling and catalyst regeneration), which are not studied here. Therefore, one should compare our findings with experimental observations with caution.

Scheme 3. Schematic Presentation of Important Variables, Computationally Investigated in This Paper, That May Impact C−H Functionalization within the [MPAA]−Pd(II)−[DG-SUB] Structural Motif

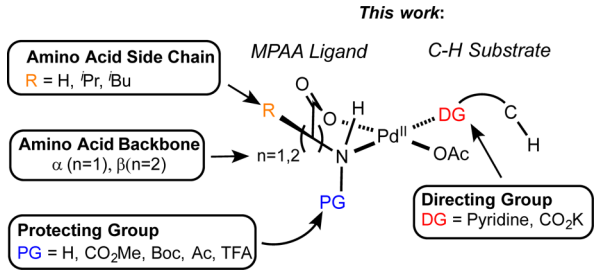

2. COMPUTATIONAL DETAILS

All calculations were performed with the Gaussian 09 (G09) program.[13] Reported geometries and energies were obtained (without geometry constraint) by using of the (B3LYP+D3) method[14] with the Lanl2dz basis set and corresponding Hay−Wadt effective core potential (ECP)[15] for Pd and standard 6-31G(d,p) basis set for all other atoms. The reported energetics and geometries incorporate solvent effects (THF is used as a solvent) calculated at the self-consistent reaction field IEF-PCM level of theory.[16] Below, this method is referred to as [B3LYP+D3]/[Lanl2dz+6-31G(d,p)] or [B3LYP+D3]/BS1. Frequency calculations are performed at the same level of theory to confirm the nature (equilibrium structure or transition state) of the reported structures and calculate enthalpy and entropy corrections to the reported energies. Intrinsic reaction coordinate (IRC) calculations were performed for representative transition states to ensure that they connect the appropriate reactant and product. Relative free energies and enthalpies, calculated under standard conditions (1 atm and 298.15 K), are reported as $\Delta G/\Delta H$ (in kcal/mol), whereas in the text, we discuss mostly relative free energies.

For specific cases indicated below, we also applied a hybrid two-layer ONIOM method, ONIOM(B3LYP:UFF)/BS1 to identify the steric (from the MM energy, E_{MM}) and electronic (from the QM energy, E_{QM}) contributions to the reported energetics.[17] For these cases, the calculated energies and optimized Cartesian coordinates at the B3LYP/BS1, ONIOM-(B3LYP:UFF)/BS1 and ONIOM(B3LYP/BS1:HF/3-21g*) levels of theory are provided in the Supporting Information as well as the employed ONIOM partitioning scheme. NBO analysis was performed for selected stationary points with the NBO program implemented in G09.[18] The strengths of donor (*i*)/acceptor (*j*) interactions are analyzed with the contributions of the second order NBO perturbation theory ($E^{(2)}_{i\rightarrow j}$).

3. RESULTS AND DISCUSSION

The discussion presented in this paper is organized as follows: First, we discuss the various factors affecting the coordination of MPAA ligand to Pd(II)−[DG-SUB], followed by an extensive analysis of the factors affecting the N−H bond cleavage and formation of reactive intermediate **I2** (or **I3**). At the next stage, we discuss the impact of the same factors on C−

DOI: 10.1021/cs5014706
ACS Catal. 2015, 5, 830−840

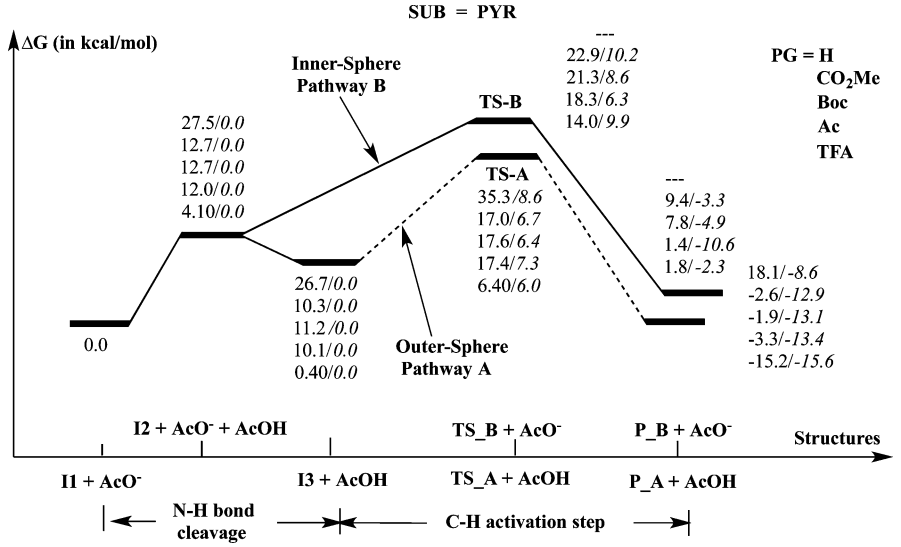

Figure 1. Protecting group (PG) effect on the potential energy surfaces for the "N−H bond cleavage and subsequent C−H bond activation" mechanism proceeding through either pathway A or B in the [MPAA′]−Pd(II)−[PYR] complex.

H bond activation in intermediate **I2** (or **I3**), and in the final section, we make several general conclusions and predictions.

3.1. MPAA Binding to Pd(II)−[DG-SUB] (i.e., the Formation of the Prereaction Complex I1). The formation of **I1** is likely a complex process that involves DG coordination, protonation of the acetate ligand by C-terminal protonated MPAA (MPAA-H), and ligand substitution. On the basis of the difference in aqueous pK_a values for the valine C-terminus (2.32) and acetic acid (4.75), the protonation event is likely favorable.[19] Furthermore, there exists literature precedence for the formation of transition metal complexes with amino acid ligands.[20] However, to account for all of the factors associated with MPAA coordination to Pd(II)−[DG-SUB], we calculated the Gibbs free energy (ΔG_{sub}) of the substitution reaction $Pd(OAc)_2$[DG-SUB] + MPAA-H → [MPAA]−Pd(OAc)[DG-SUB] + AcOH.

In all examined cases, changing side chain (R) of α-MPAA via R = H, ^{i}Pr, and ^{i}Bu has an insignificant effect on ΔG_{sub} (see the SI). For the PYR substrate, ΔG_{sub} decreases via [MPAA-H] = H-Val-OH (17.7 kcal/mol) > CO_2Me-Val-OH (6.2 kcal/mol) > Boc-Val-OH (5.4 kcal/mol) > Ac-Val-OH (4.1 kcal/mol) > TFA-Val-OH (−1.4 kcal/mol). This trend correlates with the increase in electron-withdrawing ability of the PG (H < CO_2Me ≈ Boc < Ac < TFA) and decreases the electron donating ability of the MPAA N center (N^1). In addition, the increase in length of the amino acid backbone by one carbon, that is, going from PG-(α-Val)-OH to PG-(β^2-Val)-OH, reduces ΔG_{sub} from 4.1 to 1.8 kcal/mol (for PG = Ac), which is consistent with the expected stability of the resulting five- and six-membered ring chelates, respectively.[21]

The aforementioned trends in the calculated ΔG_{sub} for SUB = PAA are the same as those reported for SUB = PYR. It decreases with the electron-withdrawing ability of the PG via [MPAA-H] = H-Val-OH (24.2 kcal/mol) > CO_2Me-Val-OH (12.8 kcal/mol) > Boc-Val-OH (12.0 kcal/mol) > Ac-Val-OH (6.8 kcal/mol) > TFA-Val-OH (2.2 kcal/mol). However, the magnitude of ΔG_{sub} is significantly higher for SUB = PAA compared with SUB = PYR because weaker coordination of the carboxylate DG of PAA (vs pyridine DG of PYR) imposes less of a trans influence. One should note that in PAA, the counterion (K^+) associated with the carboxylate DG is implicated in mediating effective carboxylate κ^1-coordination to the Pd center.[22] Therefore, it is included in our models of the PAA substrate, but the reaction conditions could dictate that it is remotely coordinated or highly solvated and dissociated from the Pd(II) complex.

Thus, the three major factors elucidated here that weaken coordination of the MPAA ligand to Pd(II)−[DG-SUB] to form prereaction complex **I1** are (1) a strong electron-withdrawing ability of the N-protecting group, (2) a longer length of the amino acid backbone of the MPAA ligand, and (3) a strong Pd−DG bonding located trans to the Pd−N^1(MPAA) bond.

3.2. N−H Bond Cleavage and Catalytic Active Pd(II) Intermediate I2 (or I3) Formation. The reactive species for C−H activation is proposed to be the [MPAA′]−Pd(II)−[DG-SUB] complex, **I2** (or **I3**).[7] As mentioned previously, deprotonation of the PG−NH group of MPAA in prereaction complex **I1**, that is, **I1** → **I2′** through NH-TS (see Scheme 2), requires a small to moderate energy barrier. However, our extensive calculations show that the N−H cleavage transition state cannot be unambiguously isolated because of the extremely small value of the barrier for the reverse reaction, that is, **I2′** → **I1**. Therefore, below, we report the N−H cleavage barrier as an energy difference between the prereaction complex **I1** and intermediate **I2**.

MPAA Side Chain (R-group) Effect. Changing the amino acid side chain (R group) via H−^{i}Pr−^{i}Bu has only a marginal impact on the estimated N−H bond cleavage energy: the calculated free energy difference for different R groups is within 0.3−1.6 kcal/mol. This is mostly because of little steric congestion around the α-carbon (see the SI).

Protecting Group Effect. As shown in Figure 1, increasing the electron-withdrawing ability of the PG (via H < CO_2Me ≈ Boc < Ac < TFA) increases the acidity of the leaving hydrogen, that is, it decreases the energy required for the N−H bond cleavage. This finding can be explained by the complex electronic and structural changes induced by deprotonation of the PG−N^1H group. Cleavage of the N^1−H bond introduces a π-donor interaction from the N^1 center to the Pd center (see Scheme 4). The Pd center is a better acceptor of this π density when the concomitant σ donation from the N^1 center is

DOI: 10.1021/cs5014706
ACS Catal. 2015, 5, 830−840

Scheme 4. Structural Changes That Occur during Deprotonation of the PG−NH Group of the MPAA Ligand

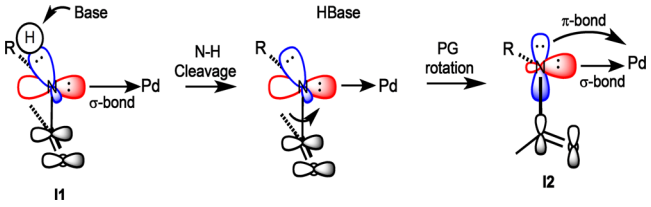

decreased as modulated by the electron-withdrawing ability of the PG. Therefore, the stability of **I2** is dependent on the stability of the nitrogen lone pair following deprotonation.

Structurally, this hypothesis is supported by (a) a rotation of the PG group around the N^1−X(PG) bond, which aligns the PG p orbitals with the N^1 lone pair (Pd−N^1−C^2−O^1 ≈ 10−15°), and (b) the Pd−N^1−C^2 angle becomes closer to 120° (see Table 1) as the electron-withdrawing ability of the PG increases, which indicates that the nitrogen has more sp^2 character.

In the case of PG = H, which has no electron-withdrawing capability or p orbitals, the formation of [MPAA′]−Pd(II)−[PYR] is highly unfavorable: the calculated N−H bond cleavage energy is 27.5 kcal/mol, and the N^1 center is in a near-sp^3 configuration with a Pd−N^1−H^2 angle of 102.6° in **I2**. Thus, the N−H bond cleavage barrier (i.e., stability of the active catalyst **I2**) is determined by the joint ability of the protecting group (PG) and Pd center to delocalize the electrons on the N^1 center of the deprotonated MPAA ligand.

Length of Amino Acid Backbone. Next, we examined the effect of the length of the amino acid backbone on the N−H cleavage step. Mono-N-protected β-amino acids (β-MPAA) contain an extra methylene group in the backbone chain between the N- and C-termini. This increases the number of possible isomers of the ligand to four. Here, to maintain consistency in the comparison of the calculated data for (β-MPAA) and (α-MPAA), we chose to study the *R* isomer of mono-N-protected β^2-valine, (*R*)-PG−(β^2-Val)−OH. This ligand places its side chain, ^{i}Pr, in a position similar to that of the α-amino acid PG−(α-Val)−OH.

The PG effect on the N−H cleavage in the β-MPAA ligands is the same as that found for α-MPAA ligands (i.e., stronger electron-withdrawing PG leads to lower N−H cleavage energy). For the sake of simplicity, here, we discuss only the PG = Ac case (for reaction energies with other PGs, see the SI). As previously mentioned, the β-MPAA ligands form a six-membered ring chelate, which assumes a boatlike conformation (see Scheme 5). In this conformation, the side chain, ^{i}Pr, is in an axial conformation, which is closer to the metal center (and consequently, to the substrate) than the α-MPAA ligands. This allows the formation of a stabilizing C−H (^{i}Pr of ligand)/π (Ph of substrate) interaction in **I2** (see Scheme 5).[23]

Scheme 5. Illustration of the Boatlike Conformation (shown in red) Assumed by the PG−(β^2-Val)−OH Ligands and the Stabilizing C−H (^{i}Pr of ligand)/π (Ph of substrate) Interaction Formed in the Active Catalyst I2[a]

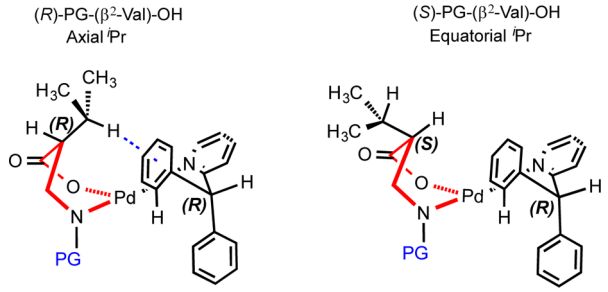

[a]Where SUB = PYR.

To further investigate the impact of the C−H (of ^{i}Pr of ligand)/π (Ph of substrate) interaction on the reaction, we also studied the ligand (*S*)-PG−(β^2-Val)−OH. In contrast to the *R* isomer, the *S* isomer places the ^{i}Pr group in an equatorial position, pointed away from the substrate and, thus, is unable to form the stabilizing C−H (^{i}Pr of ligand)/π (Ph of substrate) interaction. Consistent with this hypothesis, the **I2** intermediate

Table 1. Calculated Important Geometry Parameters of the I2 Intermediate of the N^1−H Bond Cleavage Step[a]

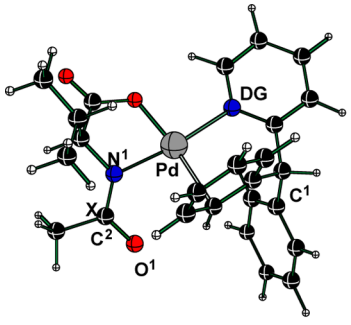

I2, PG = Ac; SUB = PYR

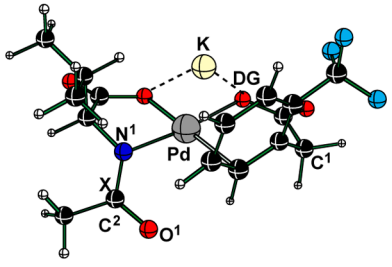

I2, PG = Ac; SUB = PAA

	SUB = PYR					SUB = PAA				
param.	H	CO_2Me	Boc	Ac	TFA	H	CO_2Me	Boc	Ac	TFA
Pd−N^1	2.00	2.00	2.01	2.01	2.03	2.01	2.00	2.00	2.01	2.01
Pd−DG	2.13	2.15	2.15	2.16	2.14	2.15	2.08	2.08	2.09	2.07
N^1−X(PG)	1.02	1.35	1.34	1.35	1.33	1.03	1.34	1.34	1.35	1.33
[Pd, N^1, X(PG)]	102.6	122.7	122.3	122.4	120.9	101.2	121.8	122.1	121.5	120.1

[a]Distances are in angstroms, and angles are in degrees. For the sake of simplicity, here, we present structures only for PG = Ac; geometry parameters for all studied PGs are provided.

DOI: 10.1021/cs5014706
ACS Catal. 2015, 5, 830−840

is found to be higher in energy by 1.8 kcal/mol for the *S* isomer of the *β*-MPAA ligand compared with its *R* isomer (see Table 2).

Table 2. Comparison of the Energies for Pathways A and B of the "N−H Bond Cleavage and Subsequent C−H Bond Activation" Mechanism for the *α*- and *β*-MPAA Ligands with the PYR Substrate

MPAA	I1	I2	I3	TS-A	TS-B	TS-A[a]	TS-B[b]
Ac-(*α*-Val)−OH	0.0	12.0	10.1	17.4	18.3	7.3	6.3
(*R*)-Ac-(*β*^{2}-Val)−OH	0.0	11.5	11.8	17.6	16.5	5.8	5.0
(*S*)-Ac-(*β*^{2}-Val)−OH	0.0	13.2	10.4	15.7	18.8	5.3	5.6

[a]Relative to intermediate **I3** [b]Relative to intermediate **I2**

One should note that the *α*-MPAA-to-*β*-MPAA substitution provides an opportunity to introduce weak, attractive, nonbonding interactions that could modulate the reactivity of the [MPAA]−Pd(II)−[DG-SUB] complex. Such weak interactions are vital but underappreciated in organic and organometallic chemistry. We will highlight the occurrence and implications of these interactions where they arise throughout the rest of the discussion.

Substrate and Directing Group Effects. Comparison of the N−H cleavage step for PAA (see Figure 2) and PYR (see Figure 1) reveals that, for a given PG, the substrate and its DG have a significant impact on the energy required for N−H cleavage. The DG of PAA (κ^1-coordinated carboxylate) imposes a weaker trans influence than that of PYR (pyridine) because it is a weaker donor. This results in an increase in the Pd−N^1 (ligand) bond energy and, consequently, an increase in the stability of **I2** for PAA compared with PYR. As seen in Figures 1 and 2, with the exception of PG = Boc, the N−H cleavage requires, in general, 3−5 kcal/mol less energy for SUB = PAA than for PYR; however, this effect is potentially limited by a steric interaction between the PG and R groups, which prevents the PG from adopting the desired planar geometry (for better interaction between N^1 and Pd). Case in point, although the PG = CO_2Me and Boc have similar electronic properties, the latter requires 2.5 kcal/mol more energy for N−H cleavage.

Thus, the data presented above show that important factors impacting the N−H cleavage step are (1) the electron-withdrawing ability of the PG; (2) the length of the amino acid backbone and the ability of the ligand and substrate to form weak, attractive interactions; and (3) the magnitude of the substrate and Pd−DG interaction through the trans influence mechanism.

3.3. The C−H Activation. As mentioned above, the C−H bond activation in the proposed "N−H bond cleavage and subsequent C−H bond activation" mechanism may proceed via two distinct pathways, A and B, starting from intermediates **I3** and **I2**, respectively. Pathway A corresponds to the outer-sphere C−H activation, where coordinated or free acetate (external) acts as a base. In contrast, pathway B corresponds to the inner-sphere C−H activation mechanisms, where the carbonyl oxygen of the PG acts as the base (see Scheme 2). For the sake of simplicity, below we discuss the transition states leading to the formation of the experimentally reported *R* stereoisomer for SUB = PYR before commenting on the source of enantioselectivity for each pathway. Representative transition state structures for PG = Ac and their geometry parameters for all PGs studied are provided in Table 3.

MPAA Side Chain (R Group) Effect. Similar to the results presented above for the N−H bond cleavage step, altering the R group via H−^{i}Pr−^{i}Bu has only minor effects on the C−H activation barriers. For pathway A, the energy of **TS-A** increases by 1−2 kcal/mol upon going from R = ^{i}Pr to R = ^{i}Bu, which can be attributed to a slight increase in steric hindrance around the substrate. However, for pathway B, energies of **TS-B** for all three studied R groups are equivalent (see the SI for energies and conformational analysis). Although these results were expected, much larger R groups may have a significant effect on the energy of the transition state of pathway A through the formation of repulsive steric or attractive noncovalent interactions (see section below).

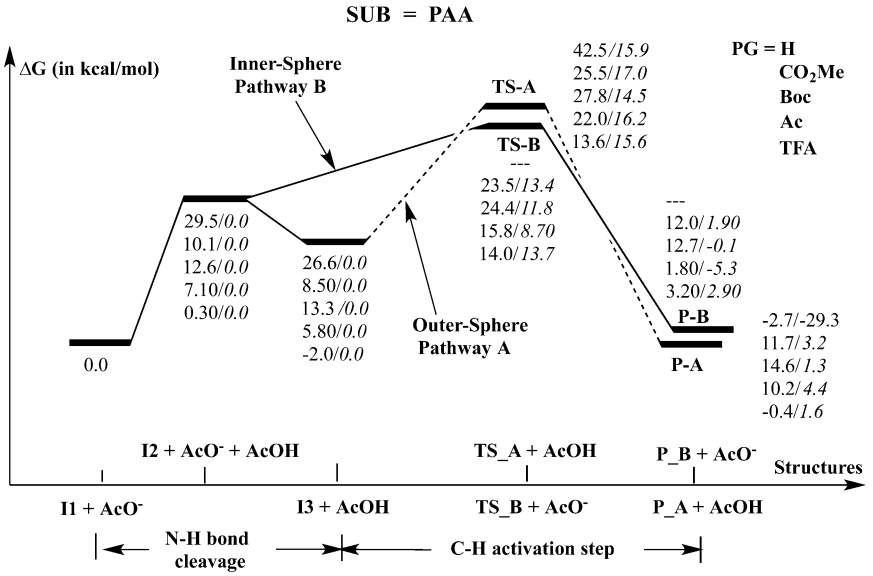

Figure 2. Protecting group (PG) effect on the potential energy surfaces for the "N−H bond cleavage and subsequent C−H bond activation" mechanism proceeding through either pathway A or B in the [MPAA′]−Pd(II)−[PAA] complex.

DOI: 10.1021/cs5014706
ACS Catal. 2015, 5, 830−840

Table 3. Calculated Important Geometry Parameters[a] of the C−H Activation Transition States TS-A and TS-B in Substrates PYR and PAA[b]

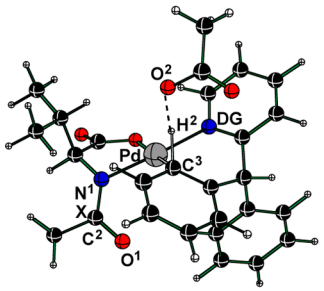

TS-A, PG = Ac; SUB = PYR

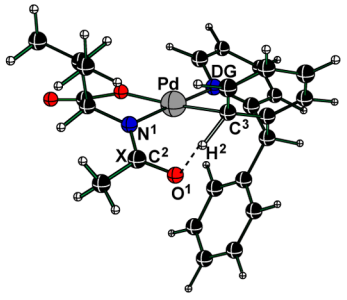

TS-B, PG = Ac; SUB = PYR

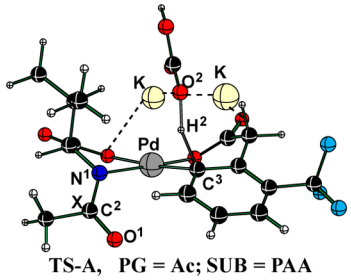

TS-A, PG = Ac; SUB = PAA

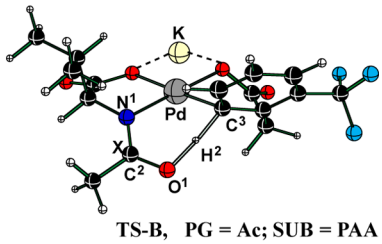

TS-B, PG = Ac; SUB = PAA

	SUB = PYR					SUB = PAA				
param.	H	CO_2Me	Boc	Ac	TFA	H	CO_2Me	Boc	Ac	TFA
outer-sphere C−H activation, **TS-A**										
$Pd-C^3$	2.18	2.19	2.19	2.19	2.19	2.11	2.14	2.15	2.13	2.14
C^3-H^2	1.29	1.23	1.24	1.24	1.23	1.42	1.36	1.38	1.39	1.38
O^3-H^2	1.39	1.47	1.46	1.46	1.48	1.30	1.34	1.31	1.30	1.30
inner-sphere C−H activation, **TS-B**										
$Pd-N^1$		2.00	2.00	2.00	2.02		2.00	2.00	2.00	2.01
$Pd-C^3$		2.15	2.16	2.17	2.15		2.14	2.14	2.15	2.13
$Pd-H^2$		2.20	2.18	2.16	2.20		2.20	2.19	2.17	2.20
C^3-H^2		1.34	1.33	1.30	1.34		1.36	1.36	1.32	1.37
O^1-H^2		1.34	1.34	1.39	1.34		1.31	1.32	1.36	1.31

[a]Distances in angstroms, and angles are in degrees. [b]For the sake of simplicity, here, we present structures only for PG = Ac; geometry parameters for all studied PG are provided.

Protecting Group Effect. As shown in Figure 1, for SUB = PYR and R = ^{i}Pr, transition state **TS-A** is lower in energy than **TS-B** for all studied protecting groups: the calculated free energy differences $\Delta\Delta G$[(**TS-B**) − (**TS-A**)] are 5.9, 3.7, 0.9, and 7.6 kcal/mol for PG = CO_2Me, Boc, Ac, and TFA, respectively. In general, for pathway A, the overall barrier decreases with the increase in the electron-withdrawing ability of the PG, which indicates that delocalization of the nitrogen lone pair remains important throughout the C−H activation reaction. One should note that a contributing factor to the stability of **I3** and **TS-A** is the weak anion−π interaction between the incoming acetate base and pyridine DG. It was shown previously that metal coordination increases the π-acidity of pyridine.[24] For PG = H, both the N−H cleavage and outer-sphere C−H activation (**TS-A**) require very high energy (27.5 and 35.3 kcal/mol, respectively), which is consistent with experiments showing no C−H functionalization for the H−*N*-Val−OH and CH_3−*N*-Ala−OH amino acid ligands.[3a]

Examination of the C−H activation barriers for pathway A, calculated from **I3**, indicates that the PG has only a minor effect on the C−H activation barriers. The energy barrier for pathway B, calculated from intermediate **I2**, correlates with the expected proton affinity of the protecting group (Ac > CO_2Me, Boc, TFA). This is consistent with the direct participation of the PG in **TS-B** as a base. Furthermore, for all studied PGs, **TS-B** and **TS-A** are higher in energy than the N−H cleavage step. Thus, the C−H activation is expected to be a rate-limiting step of the proposed "N−H bond cleavage and subsequent C−H bond activation" mechanism for substrate PYR.

Enantioselectivity. Consistent with the above presented discussion, the C−H activation barriers at the transition states **TS-A** and **TS-B** are expected to control enantioselectivity of the entire C−H functionalization reaction.[7] As was shown previously for the PYR substrate, the pathway leading to *R* isomer formation is more favorable than that leading to *S* isomer formation for the both A and B pathways.[25] This computational finding is consistent with available experiments reporting the *R* isomer as the dominant product.[3a] Close examination of the transition state structures (for schematic presentations, see Scheme 6) shows that enantioselectivity achieved via pathway A is the result of steric congestion at the C−H activation transition state leading to the *S* isomer, where the amino acid side chain and the second phenyl group of the substrate can hinder the coordination of the external base. In the transition state leading to the *R* isomer, the second phenyl group of the substrate is oriented away from the incoming base

DOI: 10.1021/cs5014706
ACS Catal. 2015, 5, 830−840

Scheme 6. Stereoselectivity Models Proposed for the Pathways A and B of the C−H Activation in [MPAA′]−Pd(II)−[PYR]

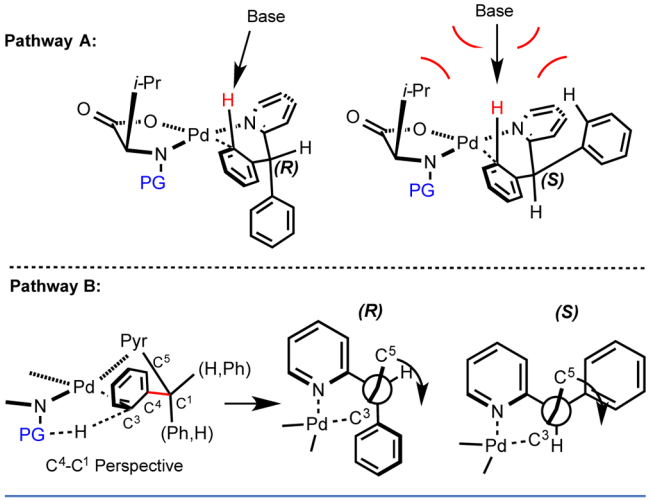

and avoids this unfavorable interaction and steric congestion. As a result, the *R* isomer formation is found to be favored (by 1.9−2.9 kcal/mol) in pathway A for all studied PG's (see Table 4), which is consistent with the experimentally observed enantioselectivity of ∼70−90% ee.[3a]

Table 4. Differences in Free Energies (in kcal/mol) of the *R* and *S* C−H activation transition states in [MPAA′]−Pd(II)−[PYR] of Pathways A and B

$\Delta\Delta G(R-S)$	CO_2Me-Val	Boc-Val	Ac-Val	TFA-Val	(*R*)-Ac-(β^2-Val)	(*S*)-Ac-(β^2-Val)
A	1.9	2.8	2.9	2.4	2.0	4.5
B	6.2	6.8	5.3	6.4	5.1	5.0

In contrast, the source of enantioselectivity in pathway B arises from the conformational preferences of the substrate. Upon formation of the new Pd−C bond in the *S* isomer, the phenyl group of the substrate must rotate, which cannot be achieved because of the near-planar coordination of the pyridine (DG), as shown in Scheme 6 (bottom). This creates unfavorable torsional strain and prevents an ideal interaction between the hydrogen of the activated C−H bond and the carbonyl oxygen of the protecting group. This is not the case for the transition state leading to formation of the *R* isomer, in which the hydrogen of the activated C−H bond occupies a more suitable position to interact with carbonyl oxygen of the protecting group. As a result, for pathway B, the *R* isomer formation becomes favored by 5.3−6.8 kcal/mol for all studied PGs (see Table 4). These energy values are a few times larger than that reported for pathway A (see above), and one should expect much higher ee values if the C−H activation proceeds via pathway B. Therefore, on the basis of the above presented analysis, we propose a cooperative ligand−substrate geometrical constraint model to explain chiral induction for pathway B.

Thus, for pathway A, enantioselectivity of the reaction arises from interactions between the amino acid R group, the substrate, and the incoming external base. In contrast, for pathway B, a cooperative ligand−substrate geometrical constraint model that is based on the lowest energy substrate conformation and torsional strain in the corresponding **TS-B** explains the observed enantioselectivity.

Length of Amino Acid Backbone. Above, we have shown that the change in length of amino acid backbone, that is, replacing α-MPAA with β-MPAA, leads to the generation of the weak, attractive, noncovalent C−H (^{i}Pr of ligand)−π (Ph of substrate) interaction with the *R* stereoisomer of the β-MPAA ligand, that is, (*R*)-PG−(β^2-Val)−OH (see Scheme 5). Existence of this noncovalent interaction results in the increase in steric congestion around the substrate and metal center and leads to an increase in the barrier for pathway A relative to pathway B (see Table 2).

We also studied the *S* stereoisomer of this ligand, (*S*)-PG−(β^2-Val)−OH, which cannot form the aforementioned stabilizing C−H (^{i}Pr of ligand)−π (Ph of substrate) interaction (see Scheme 5). It is expected that the *S* stereoisomer of β-Val will create a more sterically accessible environment around the substrate. Indeed, calculations show a trade-off between steric crowding around the substrate and the existence of the stabilizing noncovalent C−H (^{i}Pr of ligand)−π (Ph of substrate) interaction. This results in a switch of the more favorable pathway from pathway B for (*R*)-Ac-(β^2-Val)−OH to pathway A for (*S*)-Ac-(β^2-Val)−OH. The calculated energy barriers (relative to reactants **I1** + AcO^-) are 17.6 and 16.5 kcal/mol for ligand (*R*)-Ac-(β^2-Val)−OH, and 15.7 and 18.8 kcal/mol for ligand (*S*)-PG−(β^2-Val)−OH at the transition states **TS-A** and **TS-B** respectively.

The performed ONIOM calculations, including ^{i}Pr group in the lower layer and treating it at the MM level (see the SI), provide additional support to the above presented hypothesis: The calculated MM component of the activation energy ($\Delta E^{\ddagger}_{MM}$) for the ((*R*)-Ac-(β^2-Val)−OH and (*S*)-Ac-(β^2-Val)−OH ligands are 0.5 and −3.6 kcal/mol, respectively, indicating that without proper description of the noncovalent interactions, steric effects will dominate in the calculated transition state energies.

On the basis of these findings, we predict β-MPAA ligand to be a suitable and potentially advantageous ligand for C−H functionalization reactions. The design of weak, attractive, noncovalent interactions within the substrate and ligand architecture could be a powerful strategy to control reactivity and selectivity of the MPAA-assisted and DG-mediated C−H bond functionalization catalyzed by $Pd(OAc)_2$. One should emphasize that CH−π and other aromatic interactions have been previously shown to have a great influence the stereoselectivity of various organic reactions.[26]

Substrate and Directing Group Effects. An in-depth analysis of the previous findings[7,9] as well as data presented above demonstrate not only the importance of the nature of the MPAA ligand but also the nature of the substrate, strength of the Pd-DG interaction, and geometry of the ligand−substrate motif on the reactivity and selectivity of C−H activation in the [MPAA]−Pd(II)−[DG-SUB] complex.

As proposed by Wu, Houk, Yu, and co-workers, the ideal geometry for the (inner-sphere) transition state **TS-B** consists of (a) its planarity, that is, Pd−N^1−C^2−O^1 = 0°, and (b) perpendicularity of the aromatic ring of the substrate relative to the coordination plane of the Pd atom.[9] The authors used this structural concept to explain the observed regioselectivity in the MCN C−H bond activation. The substrate−ligand (MCN/Ac-Gly−OH) combination used by Houk and co-workers features a linear DG (CN), a small MPAA R-group (H), and a long linkage between the DG and substrate C−H bond and appears

DOI: 10.1021/cs5014706
ACS Catal. 2015, 5, 830−840

Scheme 7. Systematic Comparison of the Effect of (a) the PG−R Group Interaction and (b) the Substrate-Directing Group Linker on the Geometry of TS-B[a]

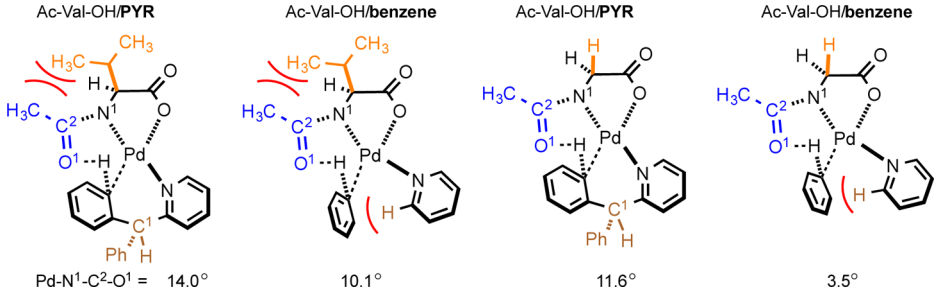

[a]PG, shown in blue; R group, shown in orange; R = *i*Pr → H; SUB = PYR and benzene, shown in brown.

to be particularly well-suited to enable the ideal TS geometry required for the inner-sphere C−H bond activation (i.e., pathway B).

In contrast, for PYR substrate and PG−Val−OH ligand (used previously,[7] as well as in this paper), the substrate−ligand geometry criteria for the transition state **TS-B** presented above are poorly fulfilled (Scheme 7). Indeed, the existing interaction between the side chain (^{i}Pr, i.e., larger R group) and PG distorts the favorable planarity of **TS-B**. Replacing PG−Val−OH with the relatively smaller ligand PG−Gly−OH (i.e., R = ^{i}Pr → H substitution) slightly increases the planarity of the TS (Pd−N^1−C^2−O^1 = 14.0° → 10.1°). It is expected that the angle imposed by the short, one-sp^3-carbon linker (C^1) between the DG and substrate also distorts the planarity of the **TS-B** and the perpendicular relationship between the substrate aromatic ring and the Pd coordination plane. To elaborate on this issue further, we also calculated the C−H activation transition state for the benzene substrate (by removing the C^1 linker). As seen in Scheme 7, the removing of the C^1 linker increases the planarity of the **TS-B** (SUB = PYR → benzene, Pd−N^1−C^2−O^1 = 14.0° → 11.6°). As might be expected, reducing the size of the R group via R = ^{i}Pr → H substitution further increases the planarity of **TS-B** with Pd−N^1−C^2−O^1 = 3.5° for the benzene substrate. However, in all studied cases, the substrate aromatic ring cannot adopt the desired perpendicular binding orientation because of the width of the strongly bound pyridine DG. Thus, the shape of the DG is also a vital determining factor for the operative pathway of the C−H activation reaction with the [MPAA′]−Pd(II)−[DG-SUB] catalyst. In short, when DG = CN (linear), pathway A is favored,[9] and when DG = pyridine (planar), pathway B is favored.

The electron-donating ability of the DG is another factor influencing the C−H activation step. In general, the calculated C−H activation barriers (for both A and B pathways) are large for substrate PAA compared with PYR. The lower C−H activation barriers for PYR can be rationalized by the coordination mode of the pyridine DG that produces a more electrophilic Pd through increased back-bonding. This is directly in competition with the trans influence observed in the active catalyst formation step and indicates an opposing effect of the DG on the N−H and C−H activation steps. Thus, the shape, interactions of the substrate and ligand, and the donating character of the DG can bias the reactivity toward either pathway and are important factors to consider in the design of enantioselective MPAA-assisted and DG-mediated C−H bond functionalization reactions catalyzed by $Pd(OAc)_2$. It should also be noted that the experimental base for the reaction with PAA is $KHCO_3$. The formation of a cation−π interaction between the base (K^+) and the substrate aryl ring may assist with association of the external base. The results with both substrates suggest that weak interactions will be important for describing the approach of the external base and therefore will have an impact on the favored pathway.

4. CONCLUSIONS

Above, we presented a computational study on the impact of experimentally relevant reaction variables, such as (a) the protecting group (PG), (b) the side chain (R), (c) the length of the amino acid backbone (α- and β-amino acid) of the MPAA ligand, as well as (d) the nature of the substrate (DG-SUB) and (e) the strength of the Pd-DG interaction on the "N−H bond cleavage and subsequent C−H bond activation" mechanism for C−H functionalization with the [MPAA]−Pd(II)−[DG-SUB] complex. Results of these studies can be summarized as follows:

(1) The major factors that lower the stability of the prereaction complex [MPAA]−Pd(II)−[DG-SUB], **I1**, are (a) the strong electron-withdrawing ability of the PG, (b) a longer amino acid backbone, and (c) a strong Pd−DG interaction.

(2) For the N−H bond cleavage and active catalyst formation, (a) alteration of the R-group via H−^{i}Pr−^{t}Bu has little impact, (b) the increase in the electron-withdrawing ability of the PG manifests in smaller N−H bond cleavage energy, (c) a change in the length of the amino acid backbone introduces the noncovalent C−H (R of ligand)−π (Ph of substrate) interaction and reduces the energy required for formation of the active catalyst, and (d) the strong Pd−DG interaction reduces the N−H cleavage energy.

(3) For C−H activation in [MPAA′]−Pd(II)−[DG-SUB], (a) alteration of the R group of MPAA has little impact, (b) the increase in the electron-withdrawing ability of PG stabilizes both pathway A (external-acetate-assisted) and pathway B (internal-acetate-assisted), (c) the existence of the weak and noncovalent C−H−π interaction between the β-MPAA ligand and substrate may alter the reaction mechanism, (d) the geometrical features (such as shape of the DG, conformational preferences of the substrate, planarity of the transition state, and the perpendicular relationship between the aromatic ring of the substrate and the coordination plane of the Pd atom) of the substrate−ligand motif provides an additional control mechanism for the reaction pathways.

DOI: 10.1021/cs5014706
ACS Catal. 2015, 5, 830−840

(4) Enantioselectivity of the reaction is controlled either through steric congestion around the substrate in pathway A or cooperative ligand−substrate geometrical constraints in pathway B.

The fundamental knowledge provided above is expected to aid the development of novel MPAA/substrate combinations and, consequently, novel synthetic strategies for the MPAA-assisted and directing group-mediated selective C−H functionalization by Pd(II) catalysts. We also wish to stress the importance of weak noncovalent interactions in the mono-N-protected amino acid ligand-assisted and directing group-mediated C−H activation catalyzed by the Pd(II) complex.

■ ASSOCIATED CONTENT

Supporting Information

The following file is available free of charge on the ACS Publications website at DOI: 10.1021/cs5014706

Three figures and nine tables showing additional experimental results; Cartesian coordinates of the reported structures (PDF)

■ AUTHOR INFORMATION

Corresponding Author

*E-mail: dmusaev@emory.edu.

Notes

The authors declare no competing financial interests.

■ ACKNOWLEDGMENTS

This work was supported by the National Science Foundation under the CCI Center for Selective C−H Functionalization (CHE-1205646). The authors gratefully acknowledge a NSF MRI-R2 Grant (CHE-0958205) and the use of the resources of the Cherry Emerson Center for Scientific Computation.

■ REFERENCES

(1) (a) Zheng, C.; You, S. L. *RSC Adv.* **2014**, *4* (12), 6173−6214. (b) Xie, J.; Pan, C.; Abdukader, A.; Zhu, C. *Chem. Soc. Rev.* **2014**, *43* (15), 5245−5256. (c) Gao, K.; Yoshikai, N. *Acc. Chem. Res.* **2014**, *47* (4), 1208−1219. (d) Yamaguchi, J.; Yamaguchi, A. D.; Itami, K. *Angew. Chem., Int. Ed.* **2012**, *51* (36), 8960−9009. (e) Li, B. J.; Shi, Z. J. *Chem. Soc. Rev.* **2012**, *41* (17), 5588−5598. (f) Kuhl, N.; Hopkinson, M. N.; Wencel-Delord, J.; Glorius, F. *Angew. Chem., Int. Ed.* **2012**, *51* (41), 10236−10254. (g) Hartwig, J. F. *Acc. Chem. Res.* **2012**, *45* (6), 864−873. (h) Doyle, M. P.; Goldberg, K. I. *Acc. Chem. Res.* **2012**, *45* (6), 777−777. (i) Arockiam, P. B.; Bruneau, C.; Dixneuf, P. H. *Chem. Rev.* **2012**, *112* (11), 5879−5918. (j) McMurray, L.; O'Hara, F.; Gaunt, M. J. *Chem. Soc. Rev.* **2011**, *40* (4), 1885−1898. (k) Davies, H. M. L.; Morton, D. *Chem. Soc. Rev.* **2011**, *40* (4), 1857−1869. (l) Davies, H. M. L.; Du Bois, J.; Yu, J. Q. *Chem. Soc. Rev.* **2011**, *40* (4), 1855−1856. (m) Cho, S. H.; Kim, J. Y.; Kwak, J.; Chang, S. *Chem. Soc. Rev.* **2011**, *40* (10), 5068−5083. (n) Boorman, T. C.; Larrosa, I. *Chem. Soc. Rev.* **2011**, *40* (4), 1910−1925. (o) Baudoin, O. *Chem. Soc. Rev.* **2011**, *40* (10), 4902−4911. (p) Lyons, T. W.; Sanford, M. S. *Chem. Rev.* **2010**, *110* (2), 1147−1169. (q) Daugulis, O.; Do, H. Q.; Shabashov, D. *Acc. Chem. Res.* **2009**, *42* (8), 1074−1086. (r) Alberico, D.; Scott, M. E.; Lautens, M. *Chem. Rev.* **2007**, *107* (1), 174−238.

(2) (a) Zhang, F.; Spring, D. R. *Chem. Soc. Rev.* **2014**, DOI: 10.1039/c4cs00137k . (b) Figg, T. M.; Park, S.; Park, J.; Chang, S.; Musaev, D. G. *Organometallics* **2014**, *33* (15), 4076−4085. (c) Ackermann, L. *Acc. Chem. Res.* **2014**, *47* (2), 281−295. (d) Rouquet, G.; Chatani, N. *Angew. Chem., Int. Ed.* **2013**, *52* (45), 11726−11743. (e) Mousseau, J. J.; Charette, A. B. *Acc. Chem. Res.* **2013**, *46* (2), 412−424. (f) Neufeldt, S. R.; Sanford, M. S. *Acc. Chem. Res.* **2012**, *45* (6), 936−946. (g) Colby, D. A.; Tsai, A. S.; Bergman, R. G.; Ellman, J. A. *Acc. Chem. Res.* **2012**, *45* (6), 814−825. (h) Seregin, I. V.; Gevorgyan, V. *Chem. Soc. Rev.* **2007**, *36* (7), 1173−1193.

(3) (a) Shi, B. F.; Maugel, N.; Zhang, Y. H.; Yu, J. Q. *Angew. Chem., Int. Ed.* **2008**, *47* (26), 4882−4886. (b) Leow, D.; Li, G.; Mei, T. S.; Yu, J. Q. *Nature* **2012**, *486* (7404), 518−522. (c) Engle, K. M.; Wang, D. H.; Yu, J. Q. *J. Am. Chem. Soc.* **2010**, *132* (40), 14137−14151.

(4) (a) Chan, K. S. L.; Wasa, M.; Chu, L.; Laforteza, B. N.; Miura, M.; Yu, J. Q. *Nat. Chem.* **2014**, *6* (2), 146−150. (b) Wasa, M.; Engle, K. M.; Lin, D. W.; Yoo, E. J.; Yu, J. Q. *J. Am. Chem. Soc.* **2011**, *133* (49), 19598−19601.

(5) (a) Yang, G. Q.; Lindovska, P.; Zhu, D. J.; Kim, J.; Wang, P.; Tang, R. Y.; Movassaghi, M.; Yu, J. Q. *J. Am. Chem. Soc.* **2014**, *136* (30), 10807−10813. (b) Gao, D. W.; Gu, Q.; You, S. L. *ACS Catal.* **2014**, *4* (8), 2741−2745. (c) Thuy-Boun, P. S.; Villa, G.; Dang, D. V.; Richardson, P.; Su, S.; Yu, J. Q. *J. Am. Chem. Soc.* **2013**, *135* (46), 17508−17513. (d) Pi, C.; Li, Y.; Cui, X. L.; Zhang, H.; Han, Y. B.; Wu, Y. J. *Chem. Sci.* **2013**, *4* (6), 2675−2679. (e) Li, G.; Leow, D. S.; Wan, L.; Yu, J. Q. *Angew. Chem., Int. Ed.* **2013**, *52* (4), 1245−1247. (f) Gao, D. W.; Shi, Y. C.; Gu, Q.; Zhao, Z. L.; You, S. L. *J. Am. Chem. Soc.* **2013**, *135* (1), 86−89. (g) Dai, H. X.; Li, G.; Zhang, X. G.; Stepan, A. F.; Yu, J. Q. *J. Am. Chem. Soc.* **2013**, *135* (20), 7567−7571. (h) Cong, X. F.; You, J. S.; Gao, G.; Lan, J. B. *Chem. Commun.* **2013**, *49* (7), 662−664. (i) Cong, X. F.; Tang, H. R.; Wu, C.; Zeng, H. M. *Organometallics* **2013**, *32* (21), 6565−6575. (j) Chu, L.; Wang, X. C.; Moore, C. E.; Rheingold, A. L.; Yu, J. Q. *J. Am. Chem. Soc.* **2013**, *135* (44), 16344−16347. (k) Cheng, X. F.; Li, Y.; Su, Y. M.; Yin, F.; Wang, J. Y.; Sheng, J.; Vora, H. U.; Wang, X. S.; Yu, J. Q. *J. Am. Chem. Soc.* **2013**, *135* (4), 1236−1239. (l) Huang, C.; Chattopadhyay, B.; Gevorgyan, V. *J. Am. Chem. Soc.* **2011**, *133* (32), 12406−12409.

(6) Xiao, K. J.; Lin, D. W.; Miura, M.; Zhu, R. Y.; Gong, W.; Wasa, M.; Yu, J. Q. *J. Am. Chem. Soc.* **2014**, *136* (22), 8138−8142.

(7) (a) Musaev, D. G.; Figg, T. M.; Kaledin, A. L. *Chem. Soc. Rev.* **2014**, *43* (14), 5009−5031. (b) Musaev, D. G.; Kaledin, A.; Shi, B. F.; Yu, J. Q. *J. Am. Chem. Soc.* **2012**, *134* (3), 1690−1698.

(8) (a) Sun, H. Y.; Gorelsky, S. I.; Stuart, D. R.; Campeau, L. C.; Fagnou, K. *J. Org. Chem.* **2010**, *75* (23), 8180−8189. (b) Pascual, S.; de Mendoza, P.; Braga, A. A. C.; Maseras, F.; Echavarren, A. M. *Tetrahedron* **2008**, *64* (26), 6021−6029. (c) Gorelsky, S. I.; Lapointe, D.; Fagnou, K. *J. Am. Chem. Soc.* **2008**, *130* (33), 10848−10849. (d) Garcia-Cuadrado, D.; de Mendoza, P.; Braga, A. A. C.; Maseras, F.; Echavarren, A. M. *J. Am. Chem. Soc.* **2007**, *129* (21), 6880−6886. (e) Lafrance, M.; Rowley, C. N.; Woo, T. K.; Fagnou, K. *J. Am. Chem. Soc.* **2006**, *128* (27), 8754−8756. (f) Garcia-Cuadrado, D.; Braga, A. A. C.; Maseras, F.; Echavarren, A. M. *J. Am. Chem. Soc.* **2006**, *128* (4), 1066−1067. (g) Davies, D. L.; Donald, S. M. A.; Macgregor, S. A. *J. Am. Chem. Soc.* **2005**, *127* (40), 13754−13755. (h) Biswas, B.; Sugimoto, M.; Sakaki, S. *Organometallics* **2000**, *19* (19), 3895−3908. (i) Gomez, M.; Granell, J.; Martinez, M. *J. Chem. Soc., Dalton Trans.* **1998**, No. 1, 37−43. (j) Gomez, M.; Granell, J.; Martinez, M. *Organometallics* **1997**, *16* (12), 2539−2546. (k) Yang, Y. F.; Cheng, G. J.; Liu, P.; Leow, D.; Sun, T. Y.; Chen, P.; Zhang, X. H.; Yu, J. Q.; Wu, Y. D.; Houk, K. N. *J. Am. Chem. Soc.* **2014**, *136* (1), 344−355.

(9) Cheng, G. J.; Yang, Y. F.; Liu, P.; Chen, P.; Sun, T. Y.; Li, G.; Zhang, X. H.; Houk, K. N.; Yu, J. Q.; Wu, Y. D. *J. Am. Chem. Soc.* **2014**, *136* (3), 894−897.

(10) Baxter, R. D.; Sale, D.; Engle, K. M.; Yu, J. Q.; Blackmond, D. G. *J. Am. Chem. Soc.* **2012**, *134* (10), 4600−4606.

(11) (a) Figg, T. M.; Wasa, M.; Yu, J. Q.; Musaev, D. G. *J. Am. Chem. Soc.* **2013**, *135* (38), 14206−14214. (b) Zhang, X. G.; Dai, H. X.; Wasa, M.; Yu, J. Q. *J. Am. Chem. Soc.* **2012**, *134* (29), 11948−11951. (c) Anand, M.; Sunoj, R. B.; Schaefer, H. F. *J. Am. Chem. Soc.* **2014**, *136* (15), 5535−5538. (d) Anand, M.; Sunoj, R. B. *Organometallics* **2012**, *31* (17), 6466−6481. (e) Anand, M.; Sunoj, R. B. *Org. Lett.* **2011**, *13* (18), 4802−4805.

(12) Possible C-H activation pathways, such as electrophilic palladation, C−H oxidative addition, and others have been shown experimentally and computationally to be unlikely and are therefore not discussed here. See references 3c, 5i, 8k, and 9.

(13) Frisch, M. J.; Trucks, G. W.; Schlegel, H. B.; Scuseria, G. E.; Robb, M. A.; Cheeseman, J. R.; Scalmani, G.; Barone, V.; Mennucci, B.; Petersson, G. A.; Nakatsuji, H.; Caricato, M.; Li, X.; Hratchian, H. P.; Izmaylov, A. F.; Bloino, J.; Zheng, G.; Sonnenberg, J. L.; Hada, M.; Ehara, M.; Toyota, K.; Fukuda, R.; Hasegawa, J.; Ishida, M.; Nakajima, T.; Honda, Y.; Kitao, O.; Nakai, H.; Vreven, T.; Montgomery, J. A., Jr.; Peralta, J. E.; Ogliaro, F.; Bearpark, M.; Heyd, J. J.; Brothers, E.; Kudin, K. N.; Staroverov, V. N.; Kobayashi, R.; Normand, J.; Raghavachari, K.; Rendell, A.; Burant, J. C.; Iyengar, S. S.; Tomasi, J.; Cossi, M.; Rega, N.; Millam, M. J.; Klene, M.; Knox, J. E.; Cross, J. B.; Bakken, V.; Adamo, C.; Jaramillo, J.; Gomperts, R.; Stratmann, R. E.; Yazyev, O.; Austin, A. J.; Cammi, R.; Pomelli, C.; Ochterski, J. W.; Martin, R. L.; Morokuma, K.; Zakrzewski, V. G.; Voth, G. A.; Salvador, P.; Dannenberg, J. J.; Dapprich, S.; Daniels, A. D.; Farkas, Ö.; Foresman, J. B.; Ortiz, J. V.; Cioslowski, J.; Fox, D. J. *Gaussian 09, Revision D.01*; Gaussian, Inc.: Wallingford, CT, 2009.

(14) (a) Grimme, S.; Antony, J.; Ehrlich, S.; Krieg, H. *J. Chem. Phys.* **2010**, *132*, 15. (b) Becke, A. D. *J. Chem. Phys.* **1993**, *98* (7), 5648−5652. (c) Miehlich, B.; Savin, A.; Stoll, H.; Preuss, H. *Chem. Phys. Lett.* **1989**, *157* (3), 200−206. (d) Lee, C. T.; Yang, W. T.; Parr, R. G. *Phys. Rev. B* **1988**, *37* (2), 785−789.

(15) (a) Hay, P. J.; Wadt, W. R. *J. Chem. Phys.* **1985**, *82* (1), 270−283. (b) Hay, P. J.; Wadt, W. R. *J. Chem. Phys.* **1985**, *82* (1), 299−310.

(16) (a) Scalmani, G.; Frisch, M. J. *J. Chem. Phys.* **2010**, *132*, 11. (b) Mennucci, B.; Tomasi, J. *J. Chem. Phys.* **1997**, *106* (12), 5151−5158. (c) Cances, E.; Mennucci, B.; Tomasi, J. *J. Chem. Phys.* **1997**, *107* (8), 3032−3041.

(17) (a) Vreven, T.; Byun, K. S.; Komaromi, I.; Dapprich, S.; Montgomery, J. A.; Morokuma, K.; Frisch, M. J. *J. Chem. Theory Comput.* **2006**, *2* (3), 815−826. (b) Dapprich, S.; Komaromi, I.; Byun, K. S.; Morokuma, K.; Frisch, M. J. *J. Mol. Struc. (Theochem)* **1999**, *461*, 1−21. (c) Cundari, T. R.; Deng, J.; Zhao, Y. *J. Mol. Struc. (Theochem)* **2003**, *632*, 121−129. (d) Lam, B. M. T.; Halfen, J. A.; Young, V. G.; Hagadorn, J. R.; Holland, P. L.; Lledos, A.; Cucurull-Sanchez, L.; Novoa, J. J.; Alvarez, S.; Tolman, W. B. *Inorg. Chem.* **2000**, *39* (18), 4059−4072.

(18) (a) Reed, A. E.; Weinstock, R. B.; Weinhold, F. *J. Chem. Phys.* **1985**, *83* (2), 735−746. (b) Reed, A. E.; Weinhold, F. *J. Chem. Phys.* **1985**, *83* (4), 1736−1740. (c) Foster, J. P.; Weinhold, F. *J. Am. Chem. Soc.* **1980**, *102* (24), 7211−7218.

(19) Lide, D. R. *CRC Handbook of Chemistry and Physics*, 75th ed.; CRC Press: Boca Raton, FL, 1995.

(20) (a) Severin, K.; Bergs, R.; Beck, W. *Angew. Chem., Int. Ed.* **1998**, *37* (12), 1635−1654. (b) Appleton, T. G. *Coord. Chem. Rev.* **1997**, *166*, 313−359. (c) Iakovidis, A.; Hadjiliadis, N. *Coord. Chem. Rev.* **1994**, *135*, 17−63.

(21) Hancock, R. D. *J. Chem. Educ.* **1992**, *69* (8), 615−621.

(22) (a) Engle, K. M.; Mei, T. S.; Wasa, M.; Yu, J. Q. *Acc. Chem. Res.* **2012**, *45* (6), 788−802. (b) Chen, X.; Engle, K. M.; Wang, D. H.; Yu, J. Q. *Angew. Chem., Int. Ed.* **2009**, *48* (28), 5094−5115. (c) Mei, T. S.; Giri, R.; Maugel, N.; Yu, J. Q. *Angew. Chem., Int. Ed.* **2008**, *47* (28), 5215−5219. (d) Giri, R.; Maugel, N.; Li, J. J.; Wang, D. H.; Breazzano, S. P.; Saunders, L. B.; Yu, J. Q. *J. Am. Chem. Soc.* **2007**, *129* (12), 3510−3511. (e) Chiong, H. A.; Pham, Q. N.; Daugulis, O. *J. Am. Chem. Soc.* **2007**, *129* (32), 9879−9884.

(23) When calculated without dispersion correction (B3LYP/BS1), this interaction is not observed (H−Ph = 2.85 vs 3.67 Å).

(24) Quinonero, D.; Frontera, A.; Deya, P. M. *ChemPhysChem* **2008**, *9* (3), 397−399.

(25) Either *R* or *S* isomer can form from the cis or trans isomers as defined previously. For PYR, the trans isomers are lower in energy due to steric interactions with the substrate and R group and are therefore considered the important structures in the enantio-determining C-H activation step. See reference 7.

(26) (a) Krenske, E. H.; Houk, K. N. *Acc. Chem. Res.* **2013**, *46* (4), 979−989. (b) Nishio, M.; Umezawa, Y.; Honda, K.; Tsuboyama, S.; Suezawa, H. *CrystEngComm* **2009**, *11* (9), 1757−1788. (c) Nishio, M. *Tetrahedron* **2005**, *61* (29), 6923−6950. (d) Jones, G. B. *Tetrahedron* **2001**, *57* (38), 7999−8016.

DOI: 10.1021/cs5014706
ACS Catal. 2015, 5, 830−840